

Finite element hybridization of port-Hamiltonian systems

Andrea Brugnoli^{a,*}, Ramy Rashad^b, Yi Zhang^b, Stefano Stramigioli^b

^aICA, Université de Toulouse, ISAE-SUPAERO, INSA, CNRS, MINES ALBI, UPS, Toulouse, France

^bRobotics and Mechatronics Department, University of Twente, The Netherlands

Abstract

In this contribution, we extend the hybridization framework for the Hodge Laplacian [Awanou et al., *Hybridization and postprocessing in finite element exterior calculus, 2023*] to port-Hamiltonian systems describing linear wave propagation phenomena. To this aim, a dual field mixed Galerkin discretization is introduced, in which one variable is approximated via conforming finite element spaces, whereas the second is completely local. This scheme is equivalent to the second order mixed Galerkin formulation and retains a discrete power balance and discrete conservation laws. The mixed formulation is also equivalent to the hybrid formulation. The hybrid system can be efficiently solved using a static condensation procedure in discrete time. The size reduction achieved thanks to the hybridization is greater than the one obtained for the Hodge Laplacian as one field is completely discarded. Numerical experiments on the 3D wave and Maxwell equations show the convergence of the method and the size reduction achieved by the hybridization.

Keywords: Port-Hamiltonian systems, Finite element exterior calculus, Hybridization, Dual field

1. Introduction

Distributed port-Hamiltonian systems were first introduced in [1] (see [2] for a comprehensive review) as an extension of Hamiltonian PDEs undergoing boundary interaction. The framework relies on a particular geometrical structure, that of a Dirac manifold [3]. The Stokes theorem allows defining appropriate boundary variables to account for the power exchange through the boundary of the spatial domain. This geometrical structure ignores the actual boundary conditions of the problem at hand and captures all admissible boundary flows. Because of the fact that Dirac manifolds are composable, port-Hamiltonian systems are closed under interconnection, and thus well suited for modular modelling of complex systems. The basic ideas behind this theory seem to be related to that of multi-symplectic structure (cf. [4, 5] on the multi-symplectic structure of wave equation and of total exterior algebra of differential form and [6] on finite element methods preserving such a structure).

The Dirac structure underlying port-Hamiltonian is characterized by the topological integration by parts formula, based on the Hodge duality of differential forms. When structure preserving numerical methods are devised this topological structure has to be preserved. The main difficulty when finite elements are used arises from the construction of a discrete Hodge star [7, 8]. For classical finite element differential forms the discrete Hodge star is a projection entailing loss of information (whereas the continuous counterpart is an isometry). This leads to a degenerate duality product of discrete forms. To solve this problem a primal dual formulation, involving dual spaces of finite elements, can be used. For classical finite elements, the duality between complete and trimmed polynomial families can be used to construct a non degenerate duality product. This is the approach used in [9], where a discontinuous Galerkin framework for port-Hamiltonian systems

*Corresponding author

Email addresses: andrea.brugnoli@isae-supaero.fr (Andrea Brugnoli), r.a.m.rashadhashem@utwente.nl (Ramy Rashad), y.zhang-13@utwente.nl (Yi Zhang), s.stramigioli@utwente.nl (Stefano Stramigioli)

is described. A recent approach exploits spline spaces forming a discrete de-Rham complex to construct Hodge dual isomorphic sequences [10]. Our previous work [11] relies on finite element exterior calculus [12] to discretize port-Hamiltonian wave like models, that are a special case of the more general Hodge wave equation (cf. [13] for an error analysis). Port-Hamiltonian systems exhibit a primal dual representation, that is here be used to embed the Hodge star into the codifferential operator. This idea is at the core of mixed finite element methods (and finite element exterior calculus), where some of the operators have a weak interpretation by means of integration by parts. The primal dual structure of wave propagation problems has been already analyzed in [14], where the connection between second order system and mixed discretization is discussed. However, the connection with exterior calculus is not discussed there, in particular concerning the Hodge duality.

The hybridization of the Hodge Laplacian has been recently presented in [15]. This framework represents the basis for the present contribution where the dual-field mixed formulation detailed in [11] is hybridized. Here to formulation is slightly modified, since the variable that does not undergo the exterior derivative is taken to be less regular, i.e. in a broken finite element space (this choice is common to other mixed formulations of wave propagation problems, see [16]). To ensure discrete conservation properties, this variable is such that a local discrete subcomplex property holds. This choice leaves untouched the properties obtained in Following the framework described in [15], the mixed Galerkin scheme is then hybridized by introducing a broken (and therefore local) multiplier, capturing the information related to the normal trace, and an unbroken global multiplier, representing the tangential trace of the regular variable. The hybrid formulation is completely equivalent to the mixed Galerkin discretization and thus retains all its properties. The general case of mixed boundary conditions is here considered. Explicit schemes, like the leapfrog scheme (also called Störmer-Verlet in the context of Hamiltonian dynamics) are typically preferred in the context of wave propagation. This is due to the fact that by introducing mass lumping strategies, the resulting system is fully explicit and no linear system has to be solved [17]. However, we are here concerned with exact preservation of the power balance as it implies preservation of the Dirac structure. For this reason, the time discretization is obtained by using the implicit midpoint method, that provides an exact discrete power balance [18, 19]. This implicit method can be directly applied to the index two differential-algebraic system arising from the hybridization procedure. The resulting system is a saddle point problem that can be efficiently solved via a static condensation procedure. This leads to a considerable reduction of the number of unknowns as only the global trace variable of the continuous field need to be solved for. Local variables can be subsequently computed in parallel, as they are completely uncoupled. Because of the peculiar structure of port-Hamiltonian systems, the size reduction obtained by means of the hybridization is even more important than the one obtained for the Hodge Laplacian in [15], as the L^2 variable, being of local nature, is completely discarded from the global problem.

The paper is organised as follows: in Sec. 2 a brief discussion of the L^2 theory of differential forms and the notation is presented. In Sec. 3 we introduce the modified mixed Galerkin formulation by making use of broken finite elements for differential forms. The hybridization of this formulation is presented in Sec. 4, where it is shown that the hybrid version is completely equivalent to the mixed formulation. In Sec. 5, the algebraic realization of the weak formulation is detailed. The reinterpretation of finite element assembly as interconnection of port-Hamiltonian descriptor system is also given. A time discrete system is obtained using the implicit midpoint method. Via static condensation the local variable are then eliminated. Section 6 presents numerical experiments for the wave and Maxwell equations in 3D. The equivalence of the mixed and hybrid formulation is verified numerically and the convergence rate of the variables is assessed.

2. Preliminaries

2.1. Smooth theory of differential forms

For sake of conciseness, we assume that the reader is familiar with the basic operators and results of exterior calculus (wedge product, exterior derivative, trace operator, Stokes theorem).

In the following M is a Riemannian manifold of dimension n . In this paper we distinguish true forms and pseudo forms. The Hodge star maps inner-oriented (or true) forms to outer-oriented (or pseudo) forms [20, 21] and vice versa. This distinction allows defining integral quantities that are orientation independent (like mass, energy, etc.). In this paper outer-oriented forms are denoted by means of a hat, i.e. $\hat{\alpha}^k \in \hat{\Omega}^k(M)$ where $\hat{\Omega}^k(M)$ is the space of outer oriented (or pseudo) forms. The Hodge- \star operator $\star : \Omega^k(M) \rightarrow \hat{\Omega}^{n-k}(M)$ is such that

$$\alpha^k \wedge \star \beta^k = (\alpha^k, \beta^k) \text{vol}, \quad \alpha^k, \beta^k \in \Omega^k(M),$$

where (α^k, β^k) is the pointwise inner product of forms and vol the standard volume form.

Differential forms of complementary degree with respect to the manifold dimension possess a natural duality product

$$(\alpha^k | \hat{\beta}^{n-k})_M := \int_M \alpha^k \wedge \hat{\beta}^{n-k}, \quad \alpha^k \in \Omega^k(M), \quad \hat{\beta}^{n-k} \in \hat{\Omega}^{n-k}(M), \quad k = 0, \dots, n. \quad (1)$$

An inner and an outer oriented forms are paired so that the resulting quantity is orientation independent. The duality product is also defined on the boundary ∂M whose orientation is inherited from the initial oriented manifold¹ M ($k = 0, \dots, n-1$)

$$\langle \text{tr } \alpha^k | \text{tr } \hat{\beta}^{n-k-1} \rangle_{\partial M} := \int_{\partial M} \text{tr } \alpha^k \wedge \text{tr } \hat{\beta}^{n-k-1}, \quad \alpha^k \in \Omega^k(M), \quad \hat{\beta}^{n-k-1} \in \hat{\Omega}^{n-k-1}(M). \quad (2)$$

Combing the Leibniz rule and the Stokes theorem, one has the integration by parts formula

$$(d\alpha | \hat{\beta})_M + (-1)^k (\alpha | d\hat{\beta})_M = \langle \text{tr } \alpha | \text{tr } \hat{\beta} \rangle_{\partial M}, \quad \alpha \in \Omega^k(M), \quad \beta \in \hat{\Omega}^{n-k-1}(M), \quad k = 0, \dots, n-1. \quad (3)$$

This duality pairing is important in port-Hamiltonian systems as it defines the power flow.

2.2. L^2 theory of differential forms

As in vector calculus, the L^2 Hilbert space of differential forms is the completion of the space of smooth forms $\Omega^k(M)$ in the norm induced by the L^2 inner product $(\cdot, \cdot)_M$. Taking d in the sense of distributions allows it to be extended to a closed, densely defined operator with domain $H\Omega^k(M)$, the space of k forms belonging to L^2 with weak derivative in L^2 . These spaces, connected by the operator d , form the de Rham domain complex. The formal adjoint of the exterior derivative with respect to the L^2 inner product is the codifferential operator $d^* : \Omega^k(M) \rightarrow \Omega^{k-1}(M)$ that satisfies the following integration by parts formula

$$(\alpha^k, d^* \beta^{k+1})_M = (d\alpha^k, \beta^{k+1})_M - \langle \text{tr } \alpha^k | \text{tr } \star \beta^{k+1} \rangle_{\partial M}, \quad \alpha \in \Omega^k(M), \quad \beta \in \Omega^{k+1}(M). \quad (4)$$

Analogously to the exterior derivative, the codifferential d^* may be also extended to a closed, densely defined operator with domain $H^* \Omega^k(M)$. The integration by parts formula (4) can be rewritten using the normal trace [15]. Given $\omega^k \in \Omega^k(M)$, its normal trace is a $k-1$ form on the boundary ∂M defined by

$$\text{tr}_n \omega^k = \star_{\partial}^{-1} \text{tr } \star \omega^k,$$

¹if M is not oriented ∂M has always a transverse orientation pointing outwards

where \star_∂ denotes the Hodge star at the boundary². The integration by parts formula (4) is then rewritten using the inner product on the boundary (denoted by $\langle \cdot, \cdot \rangle_{\partial M}$) as

$$\langle \text{tr } \alpha^k, \text{tr}_n \beta^{k+1} \rangle_{\partial M} = (\text{d} \alpha^k, \beta^{k+1})_M - (\alpha^k, \text{d}^* \beta^{k+1})_M. \quad (5)$$

In [22, 23], it is shown that the integration by parts formula (5) can be extended to $\alpha^k \in H\Omega^k(M)$ and $\beta^{k+1} \in H^*\Omega^{k+1}(M)$ and to manifolds with Lipschitz boundary. For the reader convenience, Table 1 resumes the notation used for inner and duality products over the domain M and the boundary ∂M .

	Inner product	Dual Product
Domain M	$(\alpha, \beta)_M = \int_M \alpha \wedge \star \beta$	$(\alpha \beta)_M = \int_M \alpha \wedge \beta$
Boundary ∂M	$\langle \alpha, \beta \rangle_{\partial M} = \int_{\partial M} \alpha \wedge \star_\partial \beta$	$\langle \alpha \beta \rangle_{\partial M} = \int_{\partial M} \alpha \wedge \beta$

Table 1: Inner and dual products on the domain M are denoted using round brackets (\cdot) , whereas on the boundary ∂M they are denoted using angle brackets $\langle \cdot \rangle$.

2.3. Broken Sobolev spaces and decomposition of Hilbert complexes

We briefly recall here some concepts related to decomposition of Hilbert complex, following closely [15]. Additional details over broken Sobolev spaces can be found in [24].

For simplicity, we will assume in what follows that \mathcal{T}_h is a regular mesh corresponding to the spatial manifold M . We denote single elements of \mathcal{T}_h by T . On each element the $L^2\Omega^k(T)$ and $H\Omega^k(T)$ space can be defined. In particular $H\Omega^k(T) \subset L^2\Omega^k(T)$. The space $L^2\Omega^k(\mathcal{T}_h)$ is isomorphic to $L^2(M)$ due to the properties of Lebesgue integration. The broken Sobolev spaces are the product spaces on the disjoint union $\bigsqcup_{T \in \mathcal{T}_h} T$

$$H\Omega^k(\mathcal{T}_h) := \prod_{T \in \mathcal{T}_h} H\Omega^k(T) \quad (6)$$

with inner product inherited by the Cartesian product structure. Sobolev spaces are naturally included in their broken versions $H\Omega^k(M) \hookrightarrow H\Omega^k(\mathcal{T}_h)$ by restriction over each cell. Broken versions of the differential operators are defined element-wise, i.e.

$$\text{d} : H\Omega^k(\mathcal{T}_h) \rightarrow H\Omega^{k+1}(\mathcal{T}_h) := \text{d}|_{H\Omega^k(T)} \quad \forall T \in \mathcal{T}_h.$$

Tangential and normal traces on the mesh disjoint facets $\partial\mathcal{T}_h := \bigsqcup_{T \in \mathcal{T}_h} \partial T$ are defined as traces on the boundary ∂T of each cell T . Defining $\langle \cdot, \cdot \rangle_{\partial\mathcal{T}_h} := \sum_{T \in \mathcal{T}_h} \langle \cdot, \cdot \rangle_{\partial T}$, the following integration by parts formula is readily obtained

$$(\text{d}\omega, \sigma)_{\mathcal{T}_h} - (\omega, \text{d}^*\sigma)_{\mathcal{T}_h} = \langle \text{tr } \omega, \text{tr}_n \sigma \rangle_{\partial\mathcal{T}_h}, \quad \forall \omega \in H\Omega^{k-1}(\mathcal{T}_h), \quad \sigma \in H^*\Omega^k(\mathcal{T}_h).$$

Traces of broken differential forms are double valued, as no continuity is imposed at interfaces. The following proposition, corresponding to Pr. 3.1. in [15], gives a characterization of unbroken Sobolev spaces as single-valued broken spaces.

Proposition 1. *Let \mathcal{T}_h be a Lipschitz decomposition of M then*

$$H\Omega^k(M) = \{\omega \in H\Omega^k(\mathcal{T}_h) : \langle \text{tr } \omega, \text{tr}_n \tau \rangle_{\partial\mathcal{T}_h} = 0, \quad \forall \tau \in \mathring{H}^*\Omega^{k+1}(M)\},$$

where $\mathring{H}^*\Omega^k(M) = \{\omega^k \in H^*\Omega^k(M) \mid \text{tr}_n \omega^k|_{\partial M} = 0\}$.

²The Hodge star on the boundary is constructed using the pullback of the metric at the boundary and the associated volume form

2.4. The primal-dual structure of port-Hamiltonian systems

By combining the canonical port-Hamiltonian system and its adjoint, two different formulations are deduced [11]. The variables in one system are the Hodge dual of those of the second one.

Primal system of outer oriented forms. Find $\hat{\alpha}^p : (0, T] \rightarrow \hat{\Omega}^p(M)$ and $\hat{\beta}^{p-1} : (0, T] \rightarrow \hat{\Omega}^{p-1}(M)$ such that

$$\frac{\partial}{\partial t} \begin{pmatrix} \hat{\alpha}^p \\ \hat{\beta}^{p-1} \end{pmatrix} = (-1)^p \begin{bmatrix} 0 & d \\ -d^* & 0 \end{bmatrix} \begin{pmatrix} \hat{\alpha}^p \\ \hat{\beta}^{p-1} \end{pmatrix}, \quad \begin{aligned} \text{tr} \star \hat{\alpha}^p|_{\Gamma_1} &= u_1^{q-1}, \\ (-1)^p \text{tr} \hat{\beta}^{p-1}|_{\Gamma_2} &= \hat{u}_2^{p-1}, \end{aligned} \quad (7)$$

with initial condition $\hat{\alpha}^p(0) = \hat{\alpha}_0^p$, $\hat{\beta}^{p-1}(0) = \hat{\beta}_0^{p-1}$. The collocated outputs are given by

$$y_1^{q-1} := \text{tr} \star \hat{\alpha}^p|_{\Gamma_2}, \quad \hat{y}_2^{p-1} := (-1)^p \text{tr} \hat{\beta}^{p-1}|_{\Gamma_1}. \quad (8)$$

Dual system of inner oriented forms. Find $\alpha^{q-1} : (0, T] \rightarrow \Omega^{q-1}(M)$ and $\beta^q : (0, T] \rightarrow \Omega^q(M)$ such that

$$\frac{\partial}{\partial t} \begin{pmatrix} \alpha^{q-1} \\ \beta^q \end{pmatrix} = \begin{bmatrix} 0 & d^* \\ -d & 0 \end{bmatrix} \begin{pmatrix} \alpha^{q-1} \\ \beta^q \end{pmatrix}, \quad \begin{aligned} \text{tr} \alpha^{q-1}|_{\Gamma_1} &= u_1^{q-1}, \\ (-1)^{p+q(n-q)} \text{tr} \star \beta^q|_{\Gamma_2} &= \hat{u}_2^{p-1}, \end{aligned} \quad (9)$$

with initial condition $\alpha^{q-1}(0) = \alpha_0^{q-1}$, $\beta^q(0) = \beta_0^q$. The outputs are given by

$$y_1^{q-1} := \text{tr} \alpha^{q-1}|_{\Gamma_2}, \quad y_2^{p-1} := (-1)^{p+q(n-q)} \text{tr} \star \beta^q|_{\Gamma_1}. \quad (10)$$

3. Mixed Galerkin discretization of port-Hamiltonian systems

A finite element exterior calculus discretization of (7), (9) is obtained by interpreting the codifferential weakly using integration by parts. Because of the simplified structure of port-Hamiltonian system one variable can be taken to be in L^2 and can be discretized using broken finite elements differential forms. The other variables lives in a conforming space.

3.1. Dual field mixed Galerkin discretization

Conforming finite element differential forms that constitute a subcomplex of the de Rham complex are denoted by $V_h^k \subset H\Omega^k(M)$ (for instance the trimmed polynomial family $V_h^k = \mathcal{P}^-\Omega^k(\mathcal{T}_h)$ [12] or the mimetic polynomial spaces [20, 25]). For each $T \in \mathcal{T}_h$, let $W_h^k(T) \subset H\Omega^k(T)$ be a finite subcomplex and

$$W_h^k := \prod_{T \in \mathcal{T}_h} W_h^k(T). \quad (11)$$

Then $W_h^k \subset H\Omega^k(\mathcal{T}_h)$ corresponds to the discrete space associated with variables belonging to $H\Omega^k(\mathcal{T}_h)$. In particular, conforming spaces V_h^k are naturally included in their broken counterpart $V_h^k \hookrightarrow W_h^k$. This property is crucial as it leads to a discrete power balance, as shown in Sec. 3.2.

To accomodate for the essential boundary conditions, the test functions are taken in the corresponding discrete space with boundary conditions

$$\hat{V}_h^k(\Gamma_2) := \{\hat{\omega}_h^k \in \hat{V}_h^k \mid \text{tr} \hat{\omega}_h^k|_{\Gamma_2} = 0\}, \quad V_h^k(\Gamma_1) := \{\omega_h^k \in V_h^k \mid \text{tr} \omega_h^k|_{\Gamma_1} = 0\}.$$

The discrete control spaces correspond to the restriction at the boundary of the V_h^k spaces

$$U_{1,h} = \text{tr} V_h^{q-1}|_{\Gamma_1}, \quad \hat{U}_{2,h} = \text{tr} \hat{V}_h^{p-1}|_{\Gamma_2}. \quad (12)$$

Discrete primal system. The discrete formulation for the primal system reads:

find $\hat{\alpha}_h^p \in \hat{W}_h^p$, $\hat{\beta}_h^{p-1} \in \hat{V}_h^{p-1}$ such that $(-1)^p \text{tr} \hat{\beta}_h^{p-1}|_{\Gamma_2} = \hat{u}_{2,h}^{p-1} \in U_{2,h}$ and

$$(\hat{v}_h^p, \partial_t \hat{\alpha}_h^p)_M = (-1)^p (\hat{v}_h^p, d \hat{\beta}_h^{p-1})_M, \quad \forall \hat{v}_h^p \in \hat{W}_h^p, \quad (13a)$$

$$(\hat{v}_h^{p-1}, \partial_t \hat{\beta}_h^{p-1})_M = (-1)^p \{-(d \hat{v}_h^{p-1}, \hat{\alpha}_h^p)_M + \langle \text{tr} \hat{v}_h^{p-1} | u_{1,h}^{q-1} \rangle_{\Gamma_1}\} \quad \forall \hat{v}_h^{p-1} \in \hat{V}_h^{p-1}(\Gamma_2), \quad (13b)$$

where $u_{1,h}^{q-1} \in U_{1,h}$.

Discrete dual system. The discrete dual port-Hamiltonian system is given by:
find $\alpha_h^{q-1} \in V_h^{q-1}$, $\beta_h^q \in W_h^q$ such that $\text{tr } \alpha_h^{q-1}|_{\Gamma_1} = u_{1,h}^{q-1} \in U_{1,h}$ and

$$(v_h^{q-1}, \partial_t \alpha_h^{q-1})_M = (dv_h^{q-1}, \beta_h^q)_M + (-1)^{(p-1)(q-1)} \langle \text{tr } v_h^{q-1} | \widehat{u}_{2,h}^{p-1} \rangle_{\Gamma_2}, \quad \forall v_h^{q-1} \in V_h^{q-1}(\Gamma_1), \quad (14a)$$

$$(v_h^q, \partial_t \beta_h^q)_M = -(v_h^q, d\alpha_h^{q-1})_M, \quad \forall v_h^q \in W_h^q, \quad (14b)$$

where $\widehat{u}_{2,h}^{p-1} \in \widehat{U}_{2,h}$.

Remark 1 (Equivalence with the second order formulation). *Since $dV_h^{k-1} \subset W_h^k$ for $k = \{p-1, q-1\}$, Eqs. (13a) (14b) hold in a strong sense. The mixed formulations coincides therefore with the second order formulation in time and space [14].*

3.2. Discrete power balance

The dual field mixed Galerkin discretization is capable of retaining the following discrete power balance (that characterizes the Dirac structure underlying port-Hamiltonian systems).

Proposition 2. *The primal-dual discrete port-Hamiltonian systems (13), (14) encode the following discrete power balance*

$$(-1)^{p(n-p)} (\alpha_h^{q-1} | \partial_t \widehat{\alpha}_h^p)_M + (\widehat{\beta}_h^{p-1} | \partial_t \beta_h^q)_M = \langle \widehat{y}_{2,h}^{p-1} | u_{1,h}^{q-1} \rangle_{\Gamma_1} + \langle \widehat{u}_{2,h}^{p-1} | y_{1,h}^{q-1} \rangle_{\Gamma_2}$$

Proof. The proof generalizes Pr. 5 in [11]. Since the conforming discrete spaces V_h^k form a de Rham subcomplex and conforming spaces are naturally included in their broken counterpart, two pointwise discrete conservation laws are verified, namely (13a), (14b)

$$\begin{aligned} d\widehat{V}_h^{p-1} \subset \widehat{V}_h^p &\hookrightarrow \widehat{W}_h^p, & \implies & \partial_t \widehat{\alpha}_h^p = (-1)^p d\widehat{\beta}_h^{p-1}, \\ dV_h^{q-1} \subset V_h^q &\hookrightarrow W_h^q, & & \partial_t \beta_h^q = -d\alpha_h^{q-1}. \end{aligned}$$

Taking the duality product of the first equation with $(-1)^{p(n-p)} \alpha_h^{q-1}$ and with $\widehat{\beta}_h^{p-1}$ for the second and summing over each cell leads

$$\begin{aligned} (-1)^{p(n-p)} (\alpha_h^{q-1} | \partial_t \widehat{\alpha}_h^p)_M + (\widehat{\beta}_h^{p-1} | \partial_t \beta_h^q)_M &= \sum_{T \in \mathcal{T}_h} (-1)^p (d\widehat{\beta}_h^{p-1} | \alpha_h^{q-1})_T - (\widehat{\beta}_h^{p-1} | d\alpha_h^{q-1})_T, \\ &= \sum_{T \in \mathcal{T}_h} (-1)^p \langle \text{tr } \widehat{\beta}_h^{p-1} | \text{tr } \alpha_h^{q-1} \rangle_{\partial T}, \\ &= \langle \widehat{y}_{2,h}^{p-1} | u_{1,h}^{q-1} \rangle_{\Gamma_1} + \langle \widehat{u}_{2,h}^{p-1} | y_{1,h}^{q-1} \rangle_{\Gamma_2}. \end{aligned}$$

The final equality uses the continuity property of differential forms (cf. Appendix A in [11]). \square

4. Hybridization of mixed Galerkin schemes

Let $W_h^k \subset H\Omega^k(\mathcal{T}_h)$ be defined as in (11). Conforming finite element spaces for the Sobolev spaces are given by $V_h^k = V^k \cup W_h^k$ where $V^k = H\Omega^k(M)$. We recall from [15] the broken and unbroken space of tangential traces finite element differential forms are then defined as follows

$$\begin{aligned} W_h^{k,t} &:= \{\text{tr } \omega_h^k : \omega_h^k \in W_h^k\}, \\ V_h^{k,t} &:= \{\text{tr } \omega_h^k : \omega_h^k \in V_h^k\} = V^k \cap W_h^{k,t} \\ V_h^{k,t}(\Gamma_1) &:= \{\text{tr } \omega_h^k : \omega_h^k \in V_h^k(\Gamma_1)\} = V^k(\Gamma_1) \cap W_h^{k,t}. \end{aligned}$$

For what concerns the space $W_h^{k,n}$, its discrete version is taken to be the dual space of $W_h^{k,t}$, i.e. $W_h^{k,n} = (W_h^{k,t})^*$. Since discrete tangential traces are piecewise polynomial, they are in $L^2(\partial\mathcal{T}_h)$ and so $W_h^{k,n} = W_h^{k,t}$ where $\langle \cdot, \cdot \rangle_{\partial\mathcal{T}_h}$ is the L^2 inner product.

Primal discrete system. Consider the variational problem: find

- Local variables: $\hat{\alpha}_h^p \in \widehat{W}_h^p$, $\hat{\beta}_h^{p-1} \in \widehat{W}_h^{p-1}$, $\hat{\alpha}_h^{p-1,\mathbf{n}} \in \widehat{W}_h^{p-1,\mathbf{n}}$;
- Global variables $\hat{\beta}_h^{p-1,\mathbf{t}} \in \widehat{V}_h^{p-1,\mathbf{t}}$;

such that $\hat{\beta}_h^{p-1,\mathbf{t}}|_{\Gamma_2} = \hat{u}_{2,h}^{p-1}$ and

$$\begin{aligned} (\hat{v}_h^p, \partial_t \hat{\alpha}_h^p)_{\mathcal{T}_h} &= (-1)^p (v_h^p, d\hat{\beta}_h^{p-1})_{\mathcal{T}_h}, & \forall \hat{v}_h^p \in \widehat{W}_h^p, & (15a) \\ (\hat{v}_h^{p-1}, \partial_t \hat{\beta}_h^{p-1})_{\mathcal{T}_h} &= (-1)^p \{-(d\hat{v}_h^{p-1}, \hat{\alpha}_h^p)_{\mathcal{T}_h} + \langle \text{tr } \hat{v}_h^{p-1}, \hat{\alpha}_h^{p-1,\mathbf{n}} \rangle_{\partial\mathcal{T}_h}\}, & \forall \hat{v}_h^{p-1} \in \widehat{W}_h^{p-1}, & (15b) \\ 0 &= -(-1)^p \langle \hat{v}_h^{p-1,\mathbf{n}}, \text{tr } \hat{\beta}_h^{p-1} - \hat{\beta}_h^{p-1,\mathbf{t}} \rangle_{\partial\mathcal{T}_h}, & \forall \hat{v}_h^{p-1,\mathbf{n}} \in \widehat{W}_h^{p-1,\mathbf{n}}, & (15c) \\ 0 &= (-1)^p \{ -\langle \hat{v}_h^{p-1,\mathbf{t}}, \hat{\alpha}_h^{p-1,\mathbf{n}} \rangle_{\partial\mathcal{T}_h} + \langle \hat{v}_h^{p-1,\mathbf{t}}, u_{1,h}^{q-1} \rangle_{\Gamma_1} \}, & \forall \hat{v}_h^{p-1,\mathbf{t}} \in \widehat{V}_h^{p-1,\mathbf{t}}(\Gamma_2). & (15d) \end{aligned}$$

Dual discrete system. Consider the variational problem: find

- Local variables: $\alpha_h^{q-1} \in W_h^{q-1}$, $\beta_h^q \in W_h^q$, $\beta_h^{q-1,\mathbf{n}} \in W_h^{q-1,\mathbf{n}}$;
- Global variables $\alpha_h^{q-1,\mathbf{t}} \in V_h^{q-1,\mathbf{t}}$;

such that $\alpha_h^{q-1,\mathbf{t}}|_{\Gamma_1} = u_{1,h}^{q-1}$ and

$$\begin{aligned} (v_h^{q-1}, \partial_t \alpha_h^{q-1})_{\mathcal{T}_h} &= (dv_h^{q-1}, \beta_h^q)_{\mathcal{T}_h} - \langle \text{tr } v_h^{q-1}, \beta_h^{q-1,\mathbf{n}} \rangle_{\partial\mathcal{T}_h}, & \forall v_h^{q-1} \in W_h^{q-1}, & (16a) \\ (v_h^q, \partial_t \beta_h^q)_{\mathcal{T}_h} &= -(v_h^q, d\alpha_h^{q-1})_{\mathcal{T}_h}, & \forall v_h^q \in W_h^q, & (16b) \\ 0 &= \langle v_h^{q-1,\mathbf{n}}, \text{tr } \alpha_h^{q-1} - \alpha_h^{q-1,\mathbf{t}} \rangle_{\partial\mathcal{T}_h}, & \forall v_h^{q-1,\mathbf{n}} \in W_h^{q-1,\mathbf{n}}, & (16c) \\ 0 &= \langle v_h^{q-1,\mathbf{t}}, \beta_h^{q-1,\mathbf{n}} \rangle_{\partial\mathcal{T}_h} + (-1)^{(p-1)(q-1)} \langle v_h^{q-1,\mathbf{t}}, \hat{u}_{2,h}^{p-1} \rangle_{\Gamma_2}, & \forall v_h^{q-1,\mathbf{t}} \in V_h^{q-1,\mathbf{t}}(\Gamma_1). & (16d) \end{aligned}$$

Equivalence of the discrete mixed and hybrid formulation. The mixed and hybrid primal discrete formulations are equivalent. The only difference is that $\hat{\alpha}_h^{p-1,\mathbf{n}}$ (resp. $\beta_h^{q-1,\mathbf{n}}$) are not exactly equal to the normal trace of $\hat{\alpha}_h^p$ (resp. β_h^q), but only weakly [15].

Theorem 1. *For the primal system, the following are equivalent:*

- $\hat{\alpha}_h^p, \hat{\beta}_h^{p-1}, \hat{\alpha}_h^{p-1,\mathbf{n}}, \hat{\beta}_h^{p-1,\mathbf{t}}$ is a solution to (15);
- $\hat{\alpha}_h^p, \hat{\beta}_h^{p-1}$ is a solution to (13). Moreover, $\hat{\beta}_h^{p-1,\mathbf{t}} = \text{tr } \hat{\beta}_h^{p-1}$ and $\hat{\alpha}_h^{p-1,\mathbf{n}}$ is uniquely determined by (15b).

For the dual system, the following are equivalent:

- $\alpha_h^{q-1}, \beta_h^q, \beta_h^{q-1,\mathbf{n}}, \alpha_h^{q-1,\mathbf{t}}$ is a solution to (16);
- $\alpha_h^{q-1}, \beta_h^q$ is a solution to (14). Moreover, $\alpha_h^{q-1,\mathbf{t}} = \text{tr } \alpha_h^{q-1}$ and $\beta_h^{q-1,\mathbf{n}}$ is uniquely determined by (16a).

Proof. The proof will be given only for the primal system. The one for the dual system is completely analogous. Assume a solution to (15) is given. Then from the variational formulation, it follows that $\hat{\beta}_h^{p-1,\mathbf{t}} = \text{tr } \hat{\beta}_h^{p-1}$. By Pr. 1 this means that $\hat{\beta}_h^{p-1} \in \widehat{H}\Omega^{p-1}(M)$. This immediately implies (13a). Taking the test function $\hat{v}^{p-1} \in H\widehat{\Omega}^{p-1}(M, \Gamma_2)$ in (15b), the boundary term on $\partial\mathcal{T}_h$ is replaced by the contribution on the Γ_1 boundary, thus leading to (13b). Uniqueness of $\hat{\alpha}_h^{p-1,\mathbf{n}}$ follows from the fact that the broken space of normal traces is in duality with the broken space of tangential traces. \square

Remark 2. *Since the primal and dual discrete hybrid systems are equivalent to the mixed Galerkin formulations, they satisfy a discrete power balance.*

5. Algebraic realization of the discrete systems and static condensation

Given a finite element basis, the algebraic realization of the different terms in the weak formulation can be computed. Both the primal discrete system (15) and dual discrete system (16) have the following common structure

$$\begin{bmatrix} \mathbf{E}_l & \mathbf{0} \\ \mathbf{0} & \mathbf{0} \end{bmatrix} \begin{pmatrix} \dot{\mathbf{x}}_l \\ \dot{\mathbf{x}}_g \end{pmatrix} = \begin{bmatrix} \mathbf{J}_l & \mathbf{C}_{lg} \\ -\mathbf{C}_{lg}^\top & \mathbf{0} \end{bmatrix} \begin{pmatrix} \mathbf{x}_l \\ \mathbf{x}_g \end{pmatrix} + \begin{bmatrix} \mathbf{B}_l & \mathbf{0} \\ \mathbf{0} & \mathbf{B}_g \end{bmatrix} \begin{pmatrix} \mathbf{u}_l \\ \mathbf{u}_g \end{pmatrix}, \quad (17)$$

where the subscript l denotes the local variables and the subscript g denotes the global variable. Matrix \mathbf{E}_l is symmetric and positive semi-definite, while \mathbf{J}_l is skew-symmetric $\mathbf{J}_l = -\mathbf{J}_l^\top$. This structure is a particular instance of a port-Hamiltonian descriptor system of index 2 [26]. We present the detailed matrix expression of the primal and dual algebraic systems. We shall use in what follows the notation $[\mathbf{x}]_R$ to indicate the vector containing the rows of vector \mathbf{x} associated with the index set R only. In particular, we will denote the index sets corresponding to the degrees of freedom of the interior of the domain by I , and the ones associated to the subpartitions Γ_1 and Γ_2 by the same letters Γ_1, Γ_2 (with a slight abuse of notation, since these symbols are also used for the corresponding continuous states). Local matrices have as subscript the disjoint union of cells or boundaries (i.e. \mathcal{T}_h or $\partial\mathcal{T}_h$). Coupled matrices have a subscript denoting the of facets $\mathcal{F}_h = \cup_{T \in \mathcal{T}_h} \partial T$.

The primal system. For what concerns the primal system, the state and input variables are the following

$$\mathbf{x}_l = \begin{pmatrix} \hat{\boldsymbol{\alpha}}^p \\ \hat{\boldsymbol{\beta}}^{p-1} \\ \hat{\boldsymbol{\alpha}}^{p-1, n} \end{pmatrix}, \quad \mathbf{x}_g = [\hat{\boldsymbol{\beta}}^{p-1, t}]_{I \cup \Gamma_1}, \quad \begin{pmatrix} \mathbf{u}_l \\ \mathbf{u}_g \end{pmatrix} = \begin{pmatrix} \hat{\mathbf{u}}_2^{p-1} \\ \hat{\mathbf{u}}_1^{q-1} \end{pmatrix}.$$

The specific structure of the matrices appearing in (17) is given by

$$\begin{aligned} \mathbf{E}_l &= \begin{bmatrix} \mathbf{M}_{\mathcal{T}_h}^p & \mathbf{0} & \mathbf{0} \\ \mathbf{0} & \mathbf{M}_{\mathcal{T}_h}^{p-1} & \mathbf{0} \\ \mathbf{0} & \mathbf{0} & \mathbf{0} \end{bmatrix}, \quad \mathbf{J}_l = (-1)^p \begin{bmatrix} \mathbf{0} & \mathbf{D}_{\mathcal{T}_h}^{p-1} & \mathbf{0} \\ (\mathbf{D}_{\mathcal{T}_h}^{p-1})^\top & \mathbf{0} & (\mathbf{T}_{\partial\mathcal{T}_h}^{p-1})^\top \mathbf{M}_{\partial\mathcal{T}_h}^{p-1} \\ \mathbf{0} & -\mathbf{M}_{\partial\mathcal{T}_h}^{p-1} \mathbf{T}_{\partial\mathcal{T}_h}^{p-1} & \mathbf{0} \end{bmatrix}, \\ \mathbf{C}_{lg} &= (-1)^p \begin{bmatrix} \mathbf{0} \\ \mathbf{0} \\ (\hat{\boldsymbol{\Xi}}_{\mathcal{F}_h/\Gamma_2}^{p-1})^\top \mathbf{M}_{\mathcal{F}_h/\Gamma_2}^{p-1} \end{bmatrix}, \quad \mathbf{B}_l = (-1)^p \begin{bmatrix} \mathbf{0} \\ \mathbf{0} \\ (\mathbf{T}_{\Gamma_2}^{p-1})^\top \mathbf{M}_{\Gamma_2}^{p-1} \end{bmatrix}, \\ \mathbf{B}_g &= (-1)^p (\mathbf{T}_{\Gamma_1}^{p-1, t})^\top \boldsymbol{\Psi}_{\Gamma_1}^{q-1}. \end{aligned}$$

The dual system. For the dual system, the state and input variables are the following

$$\mathbf{x}_l = \begin{pmatrix} \boldsymbol{\alpha}^{q-1} \\ \boldsymbol{\beta}^q \\ \boldsymbol{\beta}^{q-1, n} \end{pmatrix}, \quad \mathbf{x}_g = [\boldsymbol{\alpha}^{q-1, t}]_{I \cup \Gamma_2}, \quad \begin{pmatrix} \mathbf{u}_l \\ \mathbf{u}_g \end{pmatrix} = \begin{pmatrix} \mathbf{u}_1^{q-1} \\ \hat{\mathbf{u}}_2^{p-1} \end{pmatrix}.$$

The matrices exhibit the following structure

$$\begin{aligned} \mathbf{E}_l &= \begin{bmatrix} \mathbf{M}_{\mathcal{T}_h}^{q-1} & \mathbf{0} & \mathbf{0} \\ \mathbf{0} & \mathbf{M}_{\mathcal{T}_h}^q & \mathbf{0} \\ \mathbf{0} & \mathbf{0} & \mathbf{0} \end{bmatrix}, \quad \mathbf{J}_l = \begin{bmatrix} \mathbf{0} & (\mathbf{D}_{\mathcal{T}_h}^{q-1})^\top & -(\mathbf{T}_{\partial\mathcal{T}_h}^{q-1})^\top \mathbf{M}_{\partial\mathcal{T}_h}^{q-1} \\ -(\mathbf{D}_{\mathcal{T}_h}^{q-1}) & \mathbf{0} & \mathbf{0} \\ \mathbf{M}_{\partial\mathcal{T}_h}^{q-1} \mathbf{T}_{\partial\mathcal{T}_h}^{q-1} & \mathbf{0} & \mathbf{0} \end{bmatrix}, \\ \mathbf{C}_{lg} &= - \begin{bmatrix} \mathbf{0} \\ \mathbf{0} \\ (\boldsymbol{\Xi}_{\mathcal{F}_h/\Gamma_1}^{q-1})^\top \mathbf{M}_{\mathcal{F}_h/\Gamma_1}^{q-1} \end{bmatrix}, \quad \mathbf{B}_l = - \begin{bmatrix} \mathbf{0} \\ \mathbf{0} \\ (\mathbf{T}_{\Gamma_1}^{p-1})^\top \mathbf{M}_{\Gamma_1}^{p-1} \end{bmatrix}, \\ \mathbf{B}_g &= (-1)^{(p-1)(q-1)} (\mathbf{T}_{\Gamma_2}^{q-1, t})^\top \boldsymbol{\Psi}_{\Gamma_2}^{p-1}. \end{aligned}$$

5.1. Time discretization and static condensation

The time discretization leads to a linear saddle point system that can be efficiently solved via static condensation [27]. Since we are interested in Hamiltonian conservative systems, conservation of energy is of utmost importance. Implicit Runge-Kutta methods based on Gauss Legendre collocation points can be used to this aim [28]. These methods are also the only collocation schemes that lead to an exact discrete energy balance in the linear case [18]. The implicit midpoint method is here used to illustrate the time discretization.

Consider a total simulation time T_{end} and a equidistant splitting given by the time step $\Delta t = T_{\text{end}}/N_t$, where N_t is the total number of simulation instants. The evaluation of a generic variable \mathbf{x} at the time instant $t^n = n\Delta t$ is denoted by \mathbf{x}^n . Consider once again system (17). The application of the implicit midpoint scheme leads to the following algebraic system

$$\begin{bmatrix} \mathbf{E}_l - \frac{\Delta t}{2} \mathbf{J}_l & -\frac{\Delta t}{2} \mathbf{C}_{lg} \\ \frac{\Delta t}{2} \mathbf{C}_{lg}^\top & \mathbf{0} \end{bmatrix} \begin{pmatrix} \mathbf{x}_l^{n+1} \\ \mathbf{x}_g^{n+1} \end{pmatrix} = \begin{bmatrix} \mathbf{E}_l + \frac{\Delta t}{2} \mathbf{J}_l & \frac{\Delta t}{2} \mathbf{C}_{lg} \\ -\frac{\Delta t}{2} \mathbf{C}_{lg}^\top & \mathbf{0} \end{bmatrix} \begin{pmatrix} \mathbf{x}_l^n \\ \mathbf{x}_g^n \end{pmatrix} + \Delta t \begin{bmatrix} \mathbf{B}_l & \mathbf{0} \\ \mathbf{0} & \mathbf{B}_g \end{bmatrix} \begin{pmatrix} \mathbf{u}_l^{n+1/2} \\ \mathbf{u}_g^{n+1/2} \end{pmatrix}.$$

This system can be rewritten as the following saddle point problem

$$\begin{bmatrix} \mathbf{A} & -\mathbf{C} \\ \mathbf{C}^\top & \mathbf{0} \end{bmatrix} \begin{pmatrix} \mathbf{x}_l \\ \mathbf{x}_g \end{pmatrix} = \begin{pmatrix} \mathbf{b}_l \\ \mathbf{b}_g \end{pmatrix}. \quad (18)$$

The application of a Schur complement leads to the following system for the global variables

$$\mathbf{C}^\top \mathbf{A}^{-1} \mathbf{C} \mathbf{x}_g = \mathbf{b}_g - \mathbf{C}^\top \mathbf{A}^{-1} \mathbf{b}_l.$$

The matrix \mathbf{A} is block diagonal and contains local information. Each block can be inverted numerically or even analytically. Furthermore by Corollary 4.3. in [29], the Schur complement $\mathbf{C}^\top \mathbf{A}^{-1} \mathbf{C}$ has a positive semidefinite symmetric part, like the original matrix. This property can be exploited to design efficient preconditioning strategies [29]. Once the global variable has been computed, the local unknown is then computed by solving the following system

$$\mathbf{x}_l = \mathbf{A}^{-1} \mathbf{b}_l + \mathbf{A}^{-1} \mathbf{C} \mathbf{x}_g.$$

This system is block diagonal and can be solved in parallel.

Remark 3 (Well-posedness of the problem). *The matrix \mathbf{A} is invertible as it is given by a saddle point matrix whose off diagonal block are full rank and \mathbf{C} matrix is full rank. These properties are a consequence of the fact that $\langle \cdot, \cdot \rangle_{\partial \mathcal{T}_h}$ is simply an L^2 inner product at the discrete level. Therefore, the algebraic system (18) is well posed.*

A major advantage when using hybridization strategies is the reduced size of the system of equations to be solved. For simplicity consider the case in which no essential boundary conditions are present (this depends on which of the two system, primal or dual, is considered). The mixed Galerkin discretization leads to a total size of $\dim W_h^k + \dim V_h^{k-1}$ with $k = \{p, q\}$, whereas the hybridization strategy condenses it to $\dim V_h^{k-1, t}$. The following result is a simple application of Th. 4.4 in [15].

Theorem 2. *When only natural boundary conditions apply, the reduction in size from the conforming discretization to the hybridized system is given by*

$$(\dim W_h^k + \dim V_h^{k-1}) - \dim V_h^{k-1, t} = \dim W_h^k + \sum_{T \in \mathcal{T}_h} \dim \mathring{W}_h^{k-1}(T), \quad (19)$$

where $\mathring{W}_h(T) := \{\omega_h \in W_h^{k-1}, \text{tr } \omega_h|_{\partial T} = 0\}$ and $k = \{p, q\}$.

Proof. The space $V_h^{k-1,t}$ is the image of V_h^{k-1} under the trace map. By the rank nullity theorem their dimensions differ by the kernel

$$\begin{aligned} \dim V_h^{k-1} - \dim V_h^{k-1,t} &= \dim\{\omega_h \in V_h^{k-1} : \text{tr } \omega_h|_{\partial\mathcal{T}_h} = 0\}, \\ &= \dim \prod_{T \in \mathcal{T}_h} \mathring{W}_h^{k-1}(T) = \sum_{T \in \mathcal{T}_h} \dim \mathring{W}_h^{k-1}(T). \end{aligned} \quad (20)$$

□

Remark 4. A different strategy for solving this problem consist in constructing a projector to eliminate the Lagrange multiplier. This idea is pursued in [30] and offers several computational advantages, in particular for the parallel time domain simulation.

6. Numerical experiments

In this section, the hybridization strategy is tested for the wave and Maxwell equations. By introducing the musical isomorphism, given by the flat \flat and the sharp operator \sharp , and the isomorphism Θ converting vector fields in $n-1$ forms, the commuting diagram in Fig. 1, that provides the link between the de Rham complex and the standard operators and Sobolev space from vector calculus, is obtained.

$$\begin{array}{ccccccc} H\Omega^0(M) & \xrightarrow{\text{d}} & H\Omega^1(M) & \xrightarrow{\text{d}} & H\Omega^2(M) & \xrightarrow{\text{d}} & H\Omega^3(M) \\ \uparrow Id & & \flat \uparrow & \downarrow \sharp & \Theta \uparrow & \downarrow \Theta^{-1} & \star^{-1} \uparrow \downarrow \star \\ H^1(M) & \xrightarrow{\text{grad}} & H^{\text{curl}}(M) & \xrightarrow{\text{curl}} & H^{\text{div}}(M) & \xrightarrow{\text{div}} & L^2(M) \end{array}$$

Figure 1: Equivalence of vector and exterior calculus Sobolev spaces.

For the discretization, the trimmed polynomial family $\mathcal{P}_s^-\Omega^k(\mathcal{T}_h)$ is used. This family corresponds to the well known continuous Galerkin (or Lagrange) elements $\mathcal{P}_s^-\Omega^0(\mathcal{T}_h) \equiv \text{CG}_s(\mathcal{T}_h)$, Nédélec of the first kind $\mathcal{P}_s^-\Omega^1(\mathcal{T}_h) \equiv \text{NED}_s^1(\mathcal{T}_h)$, Raviart-Thomas $\mathcal{P}_s^-\Omega^2(\mathcal{T}_h) \equiv \text{RT}_s(\mathcal{T}_h)$ and discontinuous Galerkin $\mathcal{P}_s^-\Omega^3(\mathcal{T}_h) \equiv \text{DG}_{s-1}(\mathcal{T}_h)$, as illustrated in Figure 2.

$$\begin{array}{ccccccc} H^1(M) & \xrightarrow{\text{grad}} & H^{\text{curl}}(M) & \xrightarrow{\text{curl}} & H^{\text{div}}(M) & \xrightarrow{\text{div}} & L^2(M) \\ \downarrow \Pi_{s,h}^{-,0} & & \downarrow \Pi_{s,h}^{-,1} & & \downarrow \Pi_{s,h}^{-,2} & & \downarrow \Pi_{s,h}^{-,3} \\ \text{CG}_s(\mathcal{T}_h) & \xrightarrow{\text{grad}} & \text{NED}_s^1(\mathcal{T}_h) & \xrightarrow{\text{curl}} & \text{RT}_s(\mathcal{T}_h) & \xrightarrow{\text{div}} & \text{DG}_{s-1}(\mathcal{T}_h) \end{array}$$

Figure 2: Equivalence between finite element differential forms and classical elements.

The finite element library FIREDRAKE [31] is used for the numerical investigation. The fire-drake version to reproduce the experiment is archived at [32]. The FIREDRAKE component Slate [33] is used to implement the local solvers and static condensation.

For what concerns the computation of the error, care has to be taken when considering normal trace variable $\omega_h^{k,n} \in W_h^{k,n} \equiv W_h^{k,t}$. Identification of $\omega_h^{k,n}$ with an element of $L^2\Omega^k(\partial\mathcal{T}_h)$ is only unique up to the annihilator $(W_h^{k,t})^\perp$ [15]. Therefore, the L^2 error has to be computed after the annihilator has been removed, which is equivalent to taking the following projection $P_h\omega_{\text{ex}}^{k,n}$ of the exact solution ω_{ex}^{k+1}

$$\langle v_h^{k,t}, P_h\omega_{\text{ex}}^{k,n} \rangle_{\partial\mathcal{T}_h} = \langle v_h^{k,t}, \omega_{\text{ex}}^{k,n} \rangle_{\partial\mathcal{T}_h}, \quad \forall v_h^{k,t} \in W_h^{k,t}. \quad (21)$$

The scaled L^2 norm over a cell boundary is given by $||| \cdot |||_{\partial K} := h_T || \cdot ||_{\partial K}$ where h_T denoted the diameter of the cell $T \in \mathcal{T}_h$. For the overall mesh, we use the notation $||| \cdot |||_{\partial\mathcal{T}_h} = \sum_{T \in \mathcal{T}_h} ||| \cdot |||_{\partial K}$.

The error for $\omega_h^{k,n}$ will then measure as

$$\text{Error } \omega_h^{k,n} = |||\omega_h^{k,n} - P_h \omega_{\text{ex}}^{k,n}|||_{\partial\mathcal{T}_h}.$$

The norm $||| \cdot |||_{\partial\mathcal{T}_h}$ is also used to measure convergence for the tangential trace $\omega_h^{k,t}$.

6.1. The wave equation in 3D

The acoustic wave equation corresponds to the case $p = 3$ and $q = 1$. The energy variables are the pressure top-form $\hat{p}^3 := \hat{\alpha}^3$ and the stress one-form $\sigma^1 := \beta^1$. The Hamiltonian is given by

$$H(\hat{p}^3, u^1) = \frac{1}{2} \int_M \hat{p}^3 \wedge \star \hat{p}^3 + \sigma^1 \wedge \star \sigma^1, \quad (22)$$

with its variational derivatives given by

$$p^0 := \delta_{\hat{p}^3} H = \star \hat{p}^3, \quad \hat{\sigma}^2 := \delta_{\sigma^1} H = \star \sigma^1, \quad (23)$$

leading to the pH system

$$\begin{bmatrix} c^{-2} & 0 \\ 0 & 0 \end{bmatrix} \begin{pmatrix} \partial_t \hat{p}^3 \\ \partial_t \sigma^1 \end{pmatrix} = - \begin{bmatrix} 0 & d \\ d & 0 \end{bmatrix} \begin{pmatrix} p^0 \\ \hat{\sigma}^2 \end{pmatrix}, \quad \begin{aligned} \text{tr } p^0|_{\Gamma_1} &= u_1^0, \\ -\text{tr } \hat{\sigma}^2|_{\Gamma_2} &= \hat{u}_2^2. \end{aligned} \quad (24)$$

where c is the speed propagation. The employment of the dual field discretization leads to the resolution of two systems:

- the primal system (15) of outer oriented variables $\hat{p}_h^3, \hat{\sigma}_h^2, \hat{p}_h^{2,n}, \hat{\sigma}_h^{2,t}$;
- the dual system (16) of inner oriented variables $p_h^0, \sigma_h^1, \sigma_h^{0,n}, p_h^{0,t}$.

6.1.1. Convergence test

in this section we assess the rate of convergence for the primal and the dual formulation. For this test, the domain is the unit cube

$$M = \{(x, y, z) \in [0, 1]^3\}.$$

The boundary sub-partitions are selected to be

$$\Gamma_1 = \{(x, y, z) | x = 0 \cup y = 0 \cup z = 0\}, \quad \Gamma_2 = \{(x, y, z) | x = 1 \cup y = 1 \cup z = 1\}.$$

A structured tetrahedral mesh \mathcal{T}_h is formed by partitioning M into $N_{\text{el}} \times N_{\text{el}} \times N_{\text{el}}$ cubes, each of which is divided into six tetrahedra. The total simulation time is 1 and the time step is taken to be $\Delta t = T_{\text{end}}/500$. The speed propagation is taken to be $c = 1$. Introducing the functions

$$g(x, y, z) = \sin(x) \sin(y) \sin(z), \quad f(t) = \frac{1}{2} t^2, \quad (25)$$

the manufactured solution of (24) is given by

$$\begin{aligned} \hat{p}_{\text{ex}}^3 &= \star g \frac{df}{dt}, & p_{\text{ex}}^0 &= g \frac{df}{dt}, \\ \sigma_{\text{ex}}^1 &= -dgf, & \hat{\sigma}_{\text{ex}}^2 &= -\star dgf, \end{aligned} \quad (26)$$

A quadratic polynomial in time is taken to ensure that the error is only due to the spatial integration. For this to be a true solution a forcing has to be introduced in the pressure equation

$$\xi_p = g \frac{d^2 f}{dt^2} - \text{div}(\text{grad } g) f. \quad (27)$$

The exact solution provides the appropriate inputs to be fed into the system

$$u_1^0 = \text{tr } p_{\text{ex}}^0|_{\Gamma_1}, \quad u_2^0 = -\text{tr } \hat{\sigma}_{\text{ex}}^2|_{\Gamma_2}. \quad (28)$$

The error is measured in the Sobolev norm or the tangential norm for the facet variables at the final time T_{end} . In Fig. 3 the convergence rate of the variables is plotted against the mesh size. It can be immediately noticed that variable $\hat{p}_h^{2,n}$ superconverges (cf. Fig. 3c). This behaviour is well known for the RT and BDM elements in the static case [34]. The other variables converge with the optimal order. For what concerns the dual system, the results are shown in Fig. 4. The L^2 tangential trace of the pressure superconverges (cf. Fig. 4d) since the pressure converges with order h^s in the H^1 . All other variables converge with optimal order. In Fig. 5, the L^2 norm of the difference between the dual representation of variables. As in the dual field continuous Galerkin formulation, the dual representation of the variables converges under h-p refinement with order h^s .

The size reduction between the continuous and hybrid formulation is reported in Tables 2, 3. For the primal formulation one only solves for 40% of the degrees of freedom when third order polynomials are used. For the dual the size reduction is way more impressive (the hybrid formulation dimension is 20% of the continuous formulation in the worst case) as the broken Nédélec space is completely discarded when hybridization is used.

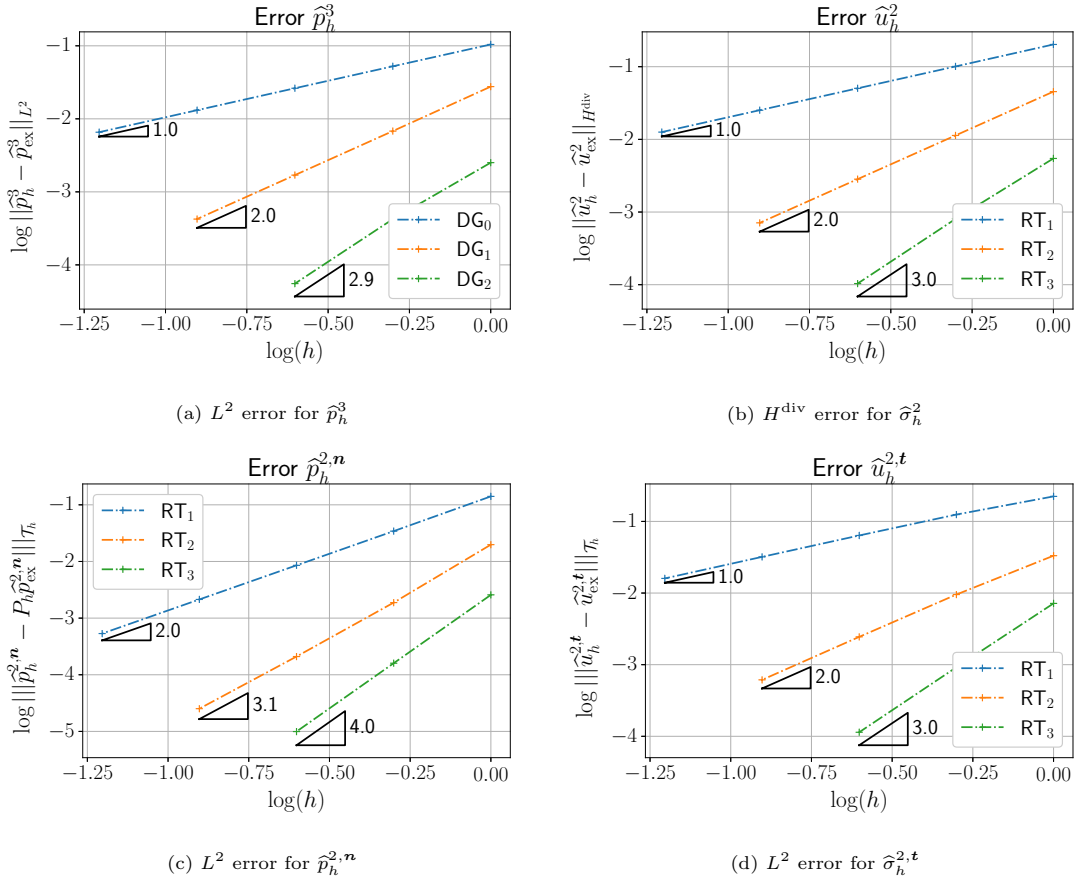
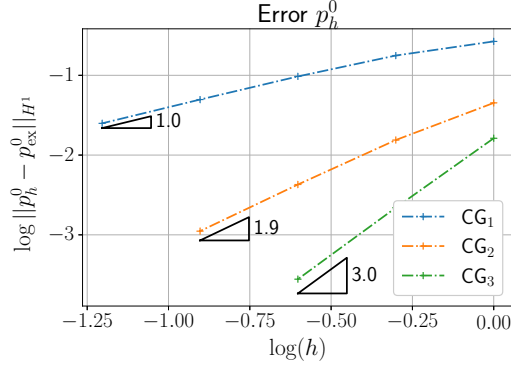
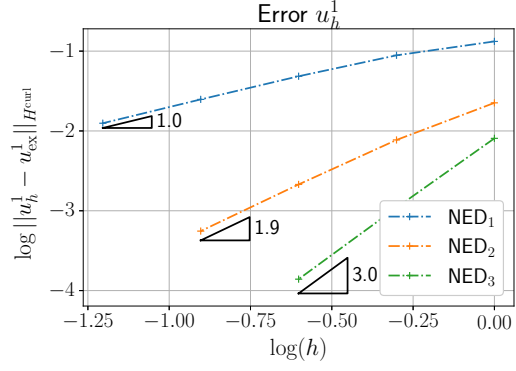


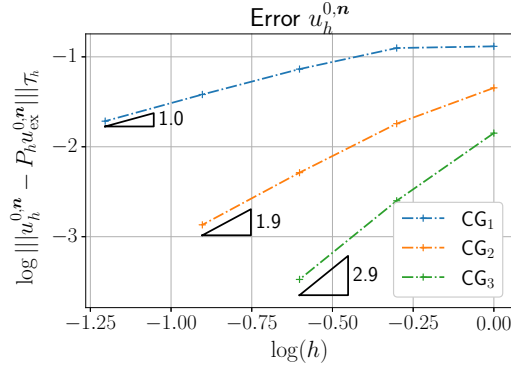
Figure 3: Convergence rate for the different variables in the primal formulation of the wave equation, measured at $T_{\text{end}} = 1$ for $\Delta t = \frac{1}{500}$.



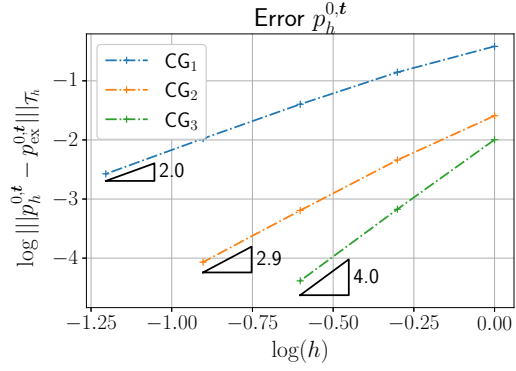
(a) H^1 error for p_h^0



(b) H^{curl} error for σ_h^1

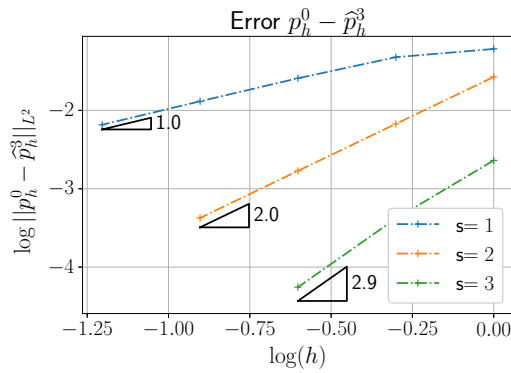


(c) L^2 error for $\sigma_h^{0,n}$

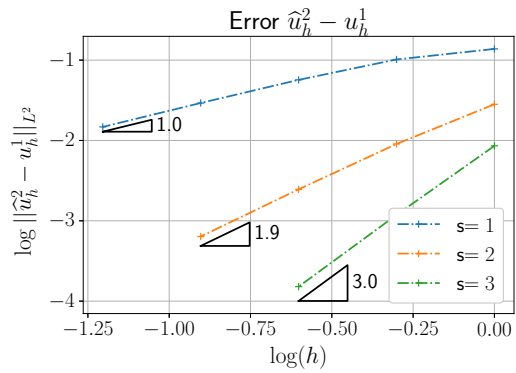


(d) L^2 error for $p_h^{0,t}$

Figure 4: Convergence rate for the different variables in the dual formulation of the wave equation, measure at at $T_{\text{end}} = 1$ for $\Delta t = \frac{1}{500}$.



(a) L^2 norm of the difference $\hat{p}_h^3 - p_h^0$



(b) L^2 norm of the difference $u_h^1 - \hat{u}_h^2$

Figure 5: L^2 difference of the dual representation of the solution for the wave equation at $T_{\text{end}} = 1$ for $\Delta t = \frac{1}{500}$.

Pol. Degree s	N_{elem}	N° dofs. continuous	N° dofs. hybrid	$N_{\text{hyb}}/N_{\text{cont}}$
1	1	24	18	75 %
	2	168	120	71%
	4	1248	864	69%
	8	9600	6528	68%
	16	75264	50688	67%
2	1	96	54	56%
	2	696	360	52%
	4	5280	2592	49%
	8	41088	19584	47%
3	1	240	108	45%
	2	1776	720	41%
	4	13632	5184	38%

Table 2: Size of the primal system \hat{p}^3, \hat{u}^2 for the wave equation: continuous and hybrid formulation.

Pol. Degree s	N_{elem}	N° dofs. continuous	N° dofs. hybrid	$N_{\text{hyb}}/N_{\text{cont}}$
1	1	44	8	18%
	2	315	27	9%
	4	2429	125	5%
	8	19161	729	4%
	16	152369	4913	3%
2	1	147	27	18%
	2	1085	125	12%
	4	8409	729	9%
	8	66353	4913	7%
3	1	334	64	19%
	2	2503	343	13%
	4	19477	2197	11%

Table 3: Size of the dual system p^0, u^1 for the wave equation: continuous and hybrid formulation.

6.1.2. An example with discontinuous coefficients

We consider the example with discontinuous coefficients [35] on the domain $M = [0, 3] \times [0, 1]$

$$c^2 = \begin{cases} 0.1 & x \leq 1, \\ 1 & x > 1. \end{cases}$$

The system is excited by the following forcing

$$\xi_p = \begin{cases} 1, & 1.2 < x < 1.4 \quad \text{and} \quad t \leq 0.2, \\ 0, & \text{else.} \end{cases}$$

Homogeneous Dirichlet conditions are considered. The system is simulated using 8192 elements and second order polynomial. The total time simulation time is $T_{\text{end}} = 4[\text{s}]$ and the time step is $\Delta t = 0.002[\text{s}]$. The snapshots, reported in Fig. 6, show the agreement between the primal and dual formulation and the different velocity speed of the front wave in the different parts of the domain.

6.2. The Maxwell equations in 3D

The Maxwell equations corresponds to the case $p = 2$, $q = 2$. The energy variables correspond to the electric displacement two form $\hat{D}^2 = \hat{\alpha}^2$ and the magnetic field $B^2 = \beta^2$. The Hamiltonian reads

$$H(\hat{D}^2, B^2) = \frac{1}{2} \int_M \hat{D}^2 \wedge \star \hat{D}^2 + B^2 \wedge \star B^2, \quad (29)$$

The variational derivative of the Hamiltonian are given by

$$E^1 := \delta_{\hat{D}^2} H = \star \hat{D}^2, \quad \hat{H}^1 := \delta_{B^2} H = \star B^2. \quad (30)$$

Variables E^1 , \hat{H}^1 are the electric field and the magnetizing field respectively. Since the reduction of the constitutive equation is such to keep only the efforts variables and their duals, the following dynamical system is obtained.

$$\begin{bmatrix} \varepsilon & 0 \\ 0 & \mu \end{bmatrix} \begin{pmatrix} \partial_t \hat{E}^2 \\ \partial_t H^2 \end{pmatrix} = \begin{bmatrix} 0 & \text{d}^1 \\ -\text{d}^1 & 0 \end{bmatrix} \begin{pmatrix} E^1 \\ \hat{H}^1 \end{pmatrix}, \quad (31)$$

where $\hat{E}^2 = \star E^1$, $H^2 = \star \hat{H}^1$ and ε , μ are the electric permittivity and magnetic permeability. The employment of the dual field discretization leads to the resolution of two systems:

- the primal system (15) of outer oriented variables $\hat{E}_h^2, \hat{H}_h^1, \hat{E}_h^{1,\mathbf{n}}, \hat{H}_h^{1,\mathbf{t}}$;
- the dual system (16) of inner oriented variables $E_h^1, H_h^2, H_h^{1,\mathbf{n}}, E_h^{1,\mathbf{t}}$.

6.2.1. Convergence results

The same mesh and boundary partitions considered in the corresponding section for the wave equation are here considered. The electric and magnetic permeability are taken to be $\varepsilon = 1$, $\mu = 1$.

Given the functions

$$\mathbf{g}(x, y, z) = \begin{pmatrix} -\cos(x) \sin(y) \sin(z) \\ 0 \\ \sin(x) \sin(y) \cos(z) \end{pmatrix}, \quad f(t) = \frac{1}{2} t^2 \quad (32)$$

The manufactured solution is given by

$$\begin{aligned} \hat{E}_{\text{ex}}^2 &= \star \mathbf{g}^b \frac{\text{d}f}{\text{d}t}, & E_{\text{ex}}^1 &= \mathbf{g}^b \frac{\text{d}f}{\text{d}t}, \\ H_{\text{ex}}^2 &= -\text{d} \mathbf{g}^b f, & \hat{H}_{\text{ex}}^1 &= -\star \text{d} \mathbf{g}^b f. \end{aligned} \quad (33)$$

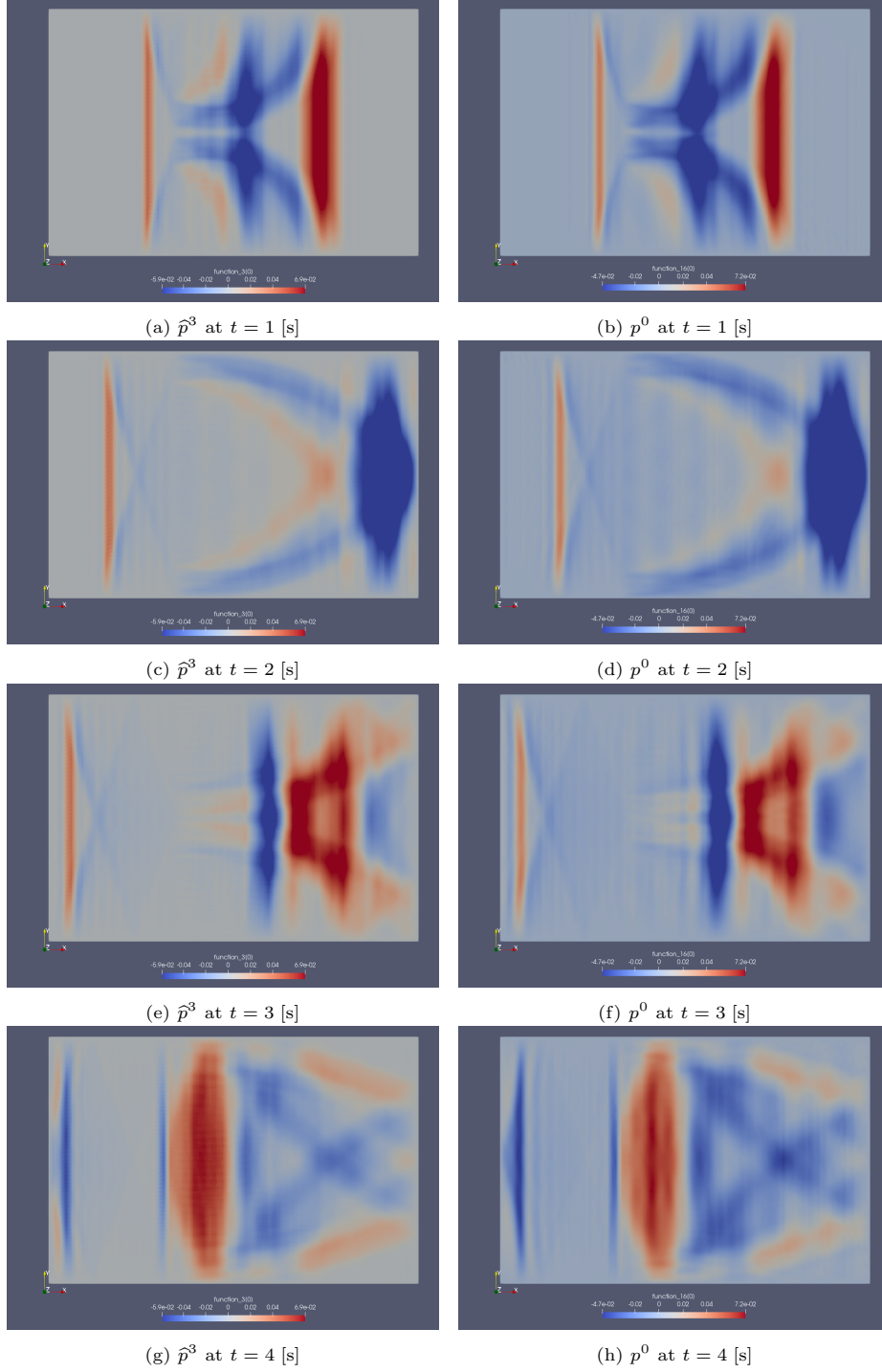


Figure 6: Snapshots of the pressure for a domain with discontinuous coefficients calculated using the primal and dual system at different time instants.

A current has to be introduced in the electric field to make this a true solution of the problem

$$j = \mathbf{g} \frac{d^2 f}{dt^2} + \text{curl curl } \mathbf{g} f.$$

The exact solution provides the appropriate inputs to be fed into the system

$$u_1^1 = \text{tr } E_{\text{ex}}^1|_{\Gamma_1}, \quad \hat{u}_2^1 = \text{tr } \hat{H}_{\text{ex}}^1|_{\Gamma_2}. \quad (34)$$

In Fig. 7 the convergence rate of the variables is plotted against the mesh size. The error is again measured in the Sobolev norm or the tangential trace norm for the facet variables at the final time T_{end} . It can be noticed that while the L^2 norm of the electric field two form converges with optimal order (cf. Fig 7a), its H^{div} norm loses one order (cf. Fig 7b). This is due to the presence of the forcing term and the fact that in FIREDRAKE the degree of freedom for Raviart Thomas are not computed via moments but instead via point normal evaluations (cf. <https://github.com/FEniCS/fiat/issues/40>). Therefore, projecting on H^{div} space does not exactly commute with the divergence. This fact entails the observed loss of convergence. All other variables converge with optimal order. The convergence results for the dual formulation are shown in Fig. 8. All variables converge with optimal as there is no forcing term in the magnetic field two form equation. In Fig. 9, the L^2 norm of the difference between the dual representation of variables. As in the dual field continuous Galerkin formulation, the dual representation of the variables converges under h-p refinement with order h^s .

The size reduction between the continuous and hybrid formulation is the same for the primal and dual system as the two formulation uses forms of the same degree and is reported in Table 4. in The hybrid system has 45% of degrees of freedom compared with the continuous formulation in the worst case. The size decreases rapidly to 30% when the number of elements and polynomial degree is increased, showing a clear computational advantage with respect to the continuous formulation presented in Sec. 3.1.

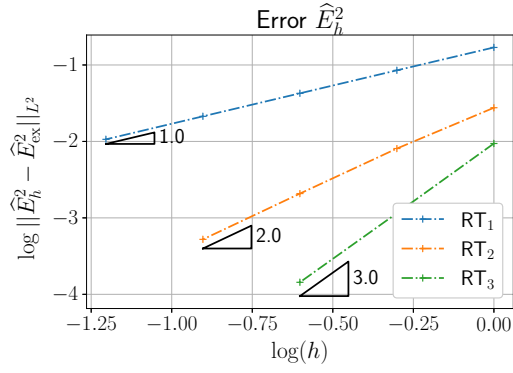
Pol. Degree s	N_{elem}	N° dofs. continuous	N° dofs. hybrid	$N_{\text{hyb}}/N_{\text{cont}}$
1	1	43	19	44%
	2	290	98	38%
	4	2140	604	28%
	8	16472	4184	25%
	16	129328	31024	24%
2	1	164	74	45%
	2	1156	436	37%
	4	8696	2936	33%
	8	67504	21424	32%
3	1	399	165	41%
	2	2886	1014	35%
	4	21972	6996	32%

Table 4: Size of the primal and dual system for the Maxwell equations: continuous and hybrid formulation.

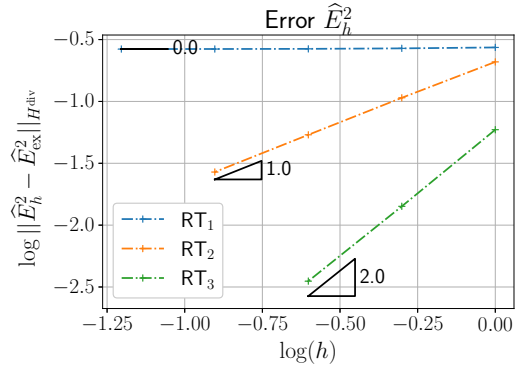
6.3. A non convex domain: the Fichera corner

As a last example, the Fichera corner geometry is considered. The domain is a cube with one octant removed $M = [-1, 1]^3 / [-1, 0]^3$. An unstructured mesh with size $h = 1/8$ and Second order Raviart-Thomas and Nédélec finite elements are used. The electric permeability and magnetic permeability $\varepsilon = 2$, $\mu = 3/2$. The following analytical solution is considered

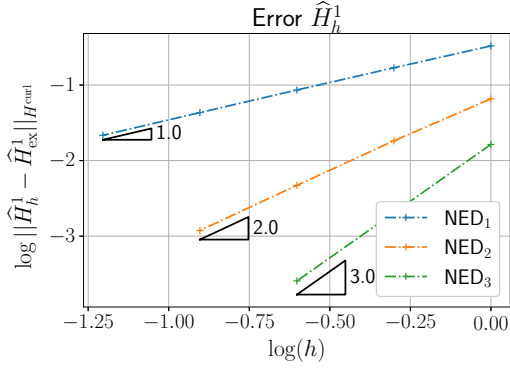
$$E = \begin{pmatrix} \sin(2t - 3z) \\ \sin(2t - 3x) \\ \sin(2t - 3y) \end{pmatrix}, \quad H = \begin{pmatrix} \sin(2t - 3y) \\ \sin(2t - 3z) \\ \sin(2t - 3x) \end{pmatrix}, \quad j = \begin{pmatrix} \cos(2t - 3z) \\ \cos(2t - 3x) \\ \cos(2t - 3y) \end{pmatrix},$$



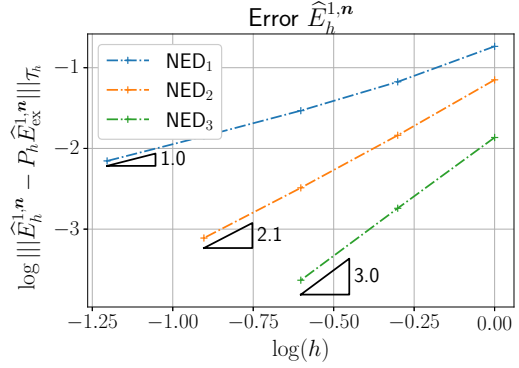
(a) L^2 error for \hat{E}_h^2



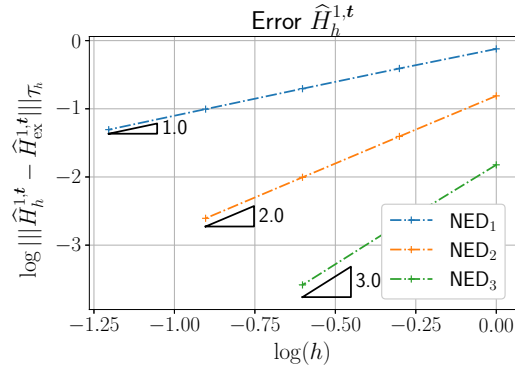
(b) H^{div} error for \hat{E}_h^2



(c) H^{curl} error for \hat{H}_h^1

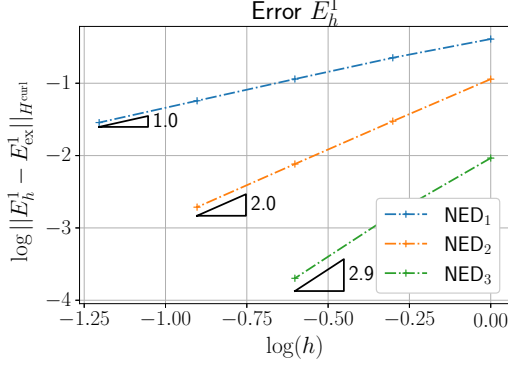


(d) L^2 error for $\hat{E}_h^{1,n}$

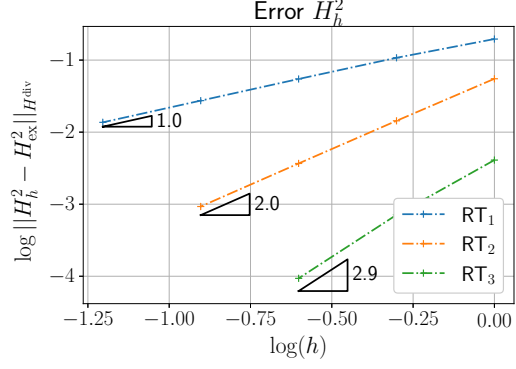


(e) L^2 error for $\hat{H}_h^{1,t}$

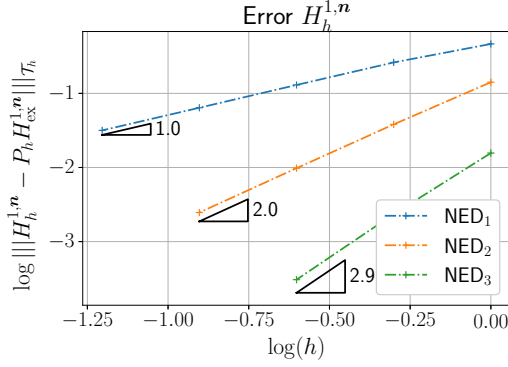
Figure 7: Convergence rate for the different variables in the primal formulation of the Maxwell equations, measured at $T_{\text{end}} = 1$ for $\Delta t = \frac{1}{500}$.



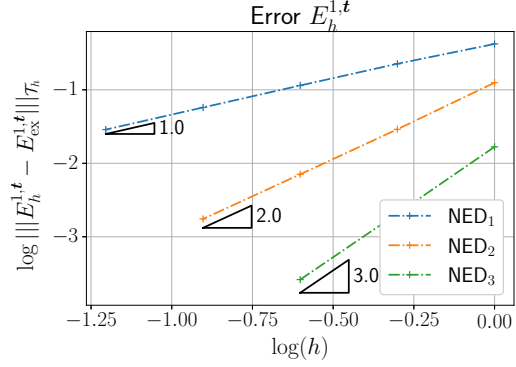
(a) H^{curl} error for E_h^1



(b) H^{div} error for H_h^2

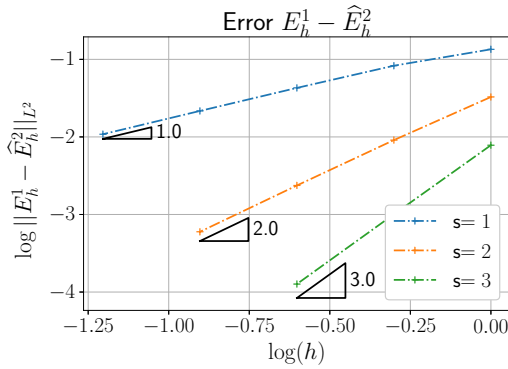


(c) L^2 error for $H_h^{1,n}$

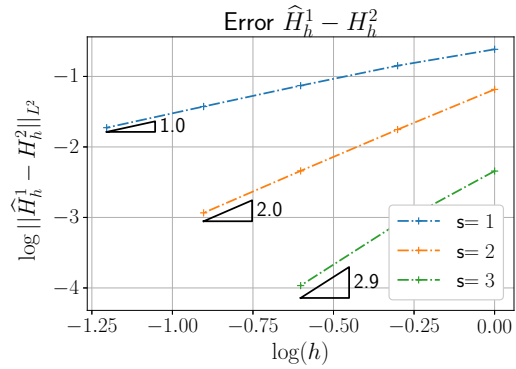


(d) L^2 error for $E_h^{1,t}$

Figure 8: Convergence rate for the different variables in the dual formulation of the Maxwell equation, measure at $T_{\text{end}} = 1$ for $\Delta t = \frac{1}{100}$.



(a) L^2 norm of the difference $\hat{E}_h^2 - E_h^1$



(b) L^2 norm of the difference $H_h^2 - \hat{H}_h^1$

Figure 9: L^2 difference of the dual representation of the solution for the Maxwell equation at $T_{\text{end}} = 1$ for $\Delta t = \frac{1}{100}$.

where a current has been introduced as a forcing to make the given solution the true one. Electric boundary conditions are considered at the boundary. The total simulation is taken to be one period of the given sinusoidal solution, i.e. $T_{\text{end}} = \pi$. The time step is taken to be $\Delta T = \pi/100$. Snapshots of the solution at the time instant $\pi/4$, $\pi/2$, $3\pi/4$, π are reported in Fig. 10. The solution is the same for the first and third snapshots as for the second and fourth, as expected from the analytical solution. A perfect agreement between primal and dual formulation is again observed.

7. Conclusion

In this work, the mixed dual field formulation is modified by taking the variable that do not undergo the exterior derivative to live in a broken finite element space. The resulting formulation is directly amenable to hybridization by introducing appropriate multipliers enforcing the continuity of the regular variable. The properties of the dual field scheme are left untouched and the hybrid formulation is highly advantageous since the broken variable, being local, is completely discarded from the global system, resulting in a huge computational gain obtained.

The first development of this work would be the employment of algebraic dual polynomials [36] to improve the condition number of the resulting matrix system. Another important topic is the employment of higher order time integration scheme and how to apply to those the static condensation procedure. The presented framework may be extended by devising post-processing schemes. This may be achieved exploiting the primal-dual structure of the equations. Furthermore, non-conforming and hybridizable discontinuous Galerkin (HDG) methods may be devised considering a more general local problem where the exterior derivative and the codifferential are taken weakly. Another important example of port-Hamiltonian system is the Elastodynamics problem. Finite element differential forms for the de Rham complex can also be used in this case but the symmetry of the stress tensor has to be enforced weakly [37]. The dual field method may be also applied to this case, by introducing an appropriate multiplier that enforces the symmetry of the stress tensor.

Code Availability

The code used for the present work is hosted at:
https://github.com/a-brugnoli/ph_hybridization.

Acknowledgements

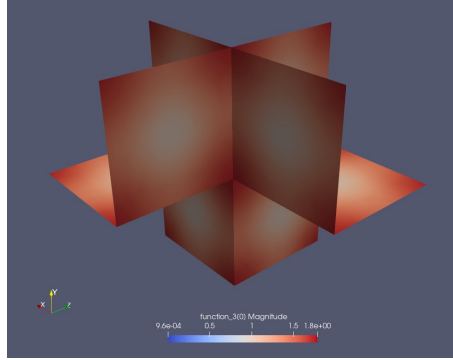
The first author would like to thank Ari Stern for sharing the code used in [15].

Funding

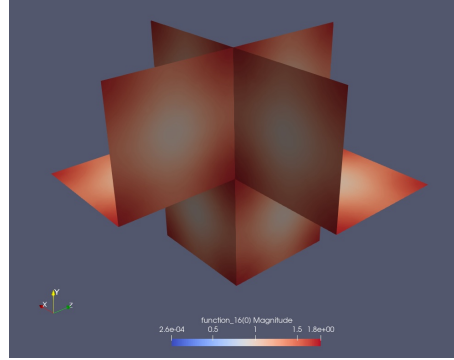
This work was supported by the PortWings project funded by the European Research Council [Grant Agreement No. 787675]

References

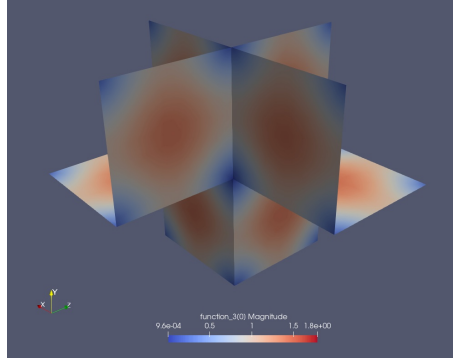
- [1] A.J. van der Schaft and B.M. Maschke. Hamiltonian formulation of distributed-parameter systems with boundary energy flow. *Journal of Geometry and Physics*, 42(1):166–194, 2002. ISSN 0393-0440. doi: 10.1016/S0393-0440(01)00083-3.
- [2] R. Rashad, F. Califano, A.J. van der Schaft, and S. Stramigioli. Twenty years of distributed port-Hamiltonian systems: a literature review. *IMA Journal of Mathematical Control and Information*, 07 2020. ISSN 1471-6887. doi: 10.1093/imamci/dnaa018.



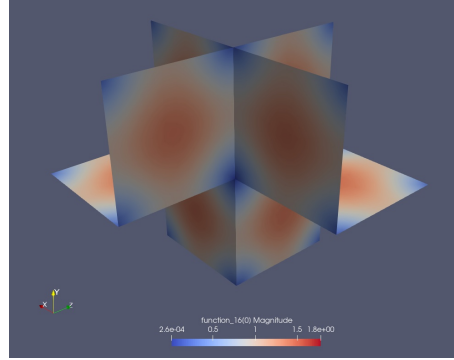
(a) $||\widehat{E}^2||$ at $t = \pi/4$ [s]



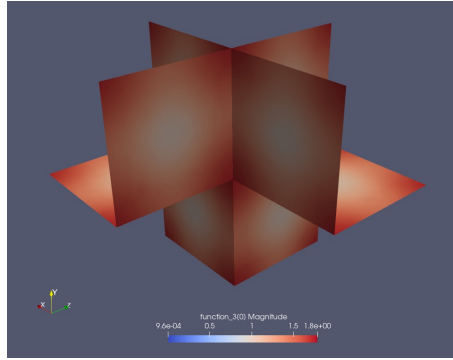
(b) $||E^1||$ at $t = \pi/4$ [s]



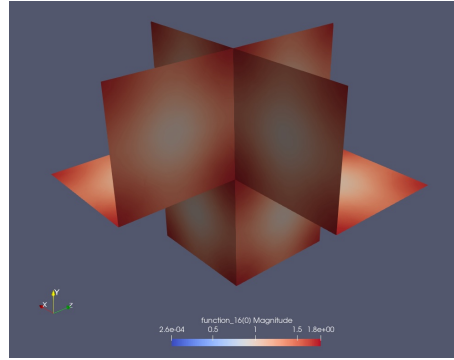
(c) $||\widehat{E}^2||$ at $t = \pi/2$ [s]



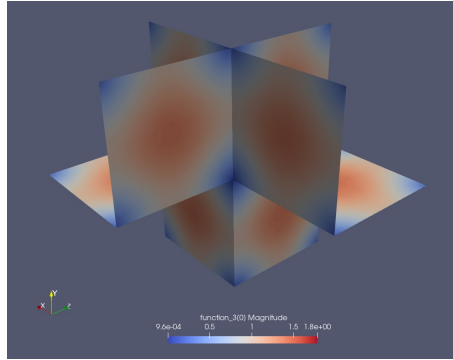
(d) $||E^1||$ at $t = \pi/2$ [s]



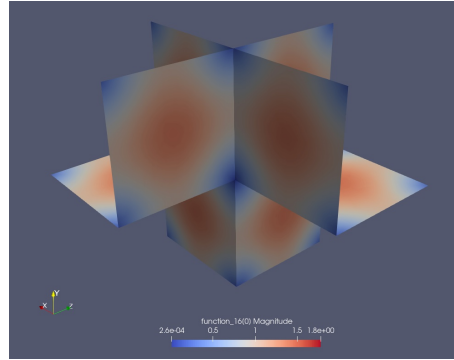
(e) $||\widehat{E}^2||$ at $t = 3\pi/4$ [s]



(f) $||E^1||$ at $t = 3\pi/4$ [s]



(g) $||\widehat{E}^2||$ at $t = \pi$ [s]



(h) $||E^1||$ at $t = \pi$ [s]

Figure 10: Snapshots of the magnitude of the electric calculated for the Fichera corner using the primal and dual system at different time instants.

- [3] Theodore James Courant. Dirac manifolds. *Transactions of the American Mathematical Society*, 319(2):631–661, 2021/12/24/ 1990. ISSN 00029947. doi: 10.2307/2001258.
- [4] Thomas J. Bridges. Multi-symplectic structures and wave propagation. *Mathematical Proceedings of the Cambridge Philosophical Society*, 121(1):147–190, 1997. doi: 10.1017/S0305004196001429.
- [5] Thomas J Bridges. Canonical multi-symplectic structure on the total exterior algebra bundle. *Proceedings of the Royal Society A: Mathematical, Physical and Engineering Sciences*, 462(2069):1531–1551, 2006. doi: 10.1098/rspa.2005.1629.
- [6] Ari Stern and Enrico Zampa. Multisymplecticity in finite element exterior calculus. *arXiv preprint arXiv:2312.03657*, 2023.
- [7] R. Hiptmair. Discrete Hodge operators. *Numerische Mathematik*, 90(2):265–289, Dec 2001. ISSN 0945-3245. doi: 10.1007/s002110100295.
- [8] Anil Nirmal Hirani. *Discrete exterior calculus*. PhD thesis, California Institute of Technology, 2003.
- [9] N Kumar, JJW van der Vegt, and HJ Zwart. Port-Hamiltonian discontinuous Galerkin finite element methods. *arXiv preprint arXiv:2212.07041*, 2022.
- [10] Bernard Kapidani and Rafael Vázquez Hernandez. High order geometric methods with splines: An analysis of discrete hodge-star operators. *SIAM Journal on Scientific Computing*, 44(6):A3673–A3699, 2022. doi: 10.1137/22M1481762.
- [11] Andrea Brugnoli, Ramy Rashad, and Stefano Stramigioli. Dual field structure-preserving discretization of port-Hamiltonian systems using finite element exterior calculus. *Journal of Computational Physics*, 471, 2022. ISSN 0021-9991. doi: 10.1016/j.jcp.2022.111601.
- [12] Douglas N. Arnold, Richard S. Falk, and Ragnar Winther. Finite element exterior calculus, homological techniques, and applications. *Acta Numerica*, 15:1–155, 2006. doi: 10.1017/S0962492906210018.
- [13] Yongke Wu and Yanhong Bai. Error analysis of energy-preserving mixed finite element methods for the hodge wave equation. *SIAM Journal on Numerical Analysis*, 59(3):1433–1454, 2021. doi: 10.1137/19M1307950.
- [14] Patrick Joly. *Variational Methods for Time-Dependent Wave Propagation Problems*, pages 201–264. Springer Berlin Heidelberg, Berlin, Heidelberg, 2003. ISBN 978-3-642-55483-4. doi: 10.1007/978-3-642-55483-4_6.
- [15] Johnny Guzmán Gerard Awanou, Maurice Fabien and Ari Stern. Hybridization and postprocessing in finite element exterior calculus. *Mathematics of Computation*, 92:79–115, 2023.
- [16] Gary C. Cohen. *Higher-order numerical methods for transient wave equations*, volume 5. Springer, 2002.
- [17] Herbert Egger and Bogdan Radu. A second-order finite element method with mass lumping for maxwell’s equations on tetrahedra. *SIAM Journal on Numerical Analysis*, 59(2):864–885, 2021. doi: 10.1137/20M1318912.
- [18] Paul Kotyczka and Laurent Lefèvre. Discrete-time port-Hamiltonian systems: A definition based on symplectic integration. *Systems & Control Letters*, 133:104530, 2019. ISSN 0167-6911. doi: 10.1016/j.sysconle.2019.104530.
- [19] Robert C. Kirby and Thinh Tri Kieu. Symplectic-mixed finite element approximation of linear acoustic wave equations. *Numerische Mathematik*, 130(2):257–291, Jun 2015. ISSN 0945-3245. doi: 10.1007/s00211-014-0667-4.

- [20] Jasper Kreeft, Artur Palha, and Marc Gerritsma. Mimetic framework on curvilinear quadrilaterals of arbitrary order. *arXiv preprint arXiv:1111.4304*, 2011.
- [21] Theodore Frankel. *The geometry of physics: an introduction*. Cambridge university press, third edition, 2011.
- [22] Norbert Weck. Traces of differential forms on Lipschitz boundaries. *Analysis*, 24(2):147–170, 2004. doi: 10.1524/anly.2004.24.14.147.
- [23] Erick Schulz. *Boundary Integral Exterior Calculus*. PhD thesis, ETH Zurich, 2022.
- [24] Constantin Bacuta, Leszek Demkowicz, Jaime Mora, and Christos Xenophontos. Analysis of non-conforming dpg methods on polyhedral meshes using fractional sobolev norms. *Computers & Mathematics with Applications*, 95:215–241, 2021. ISSN 0898-1221. doi: 10.1016/j.camwa.2020.09.018.
- [25] Artur Palha, Pedro Pinto Rebelo, René Hiemstra, Jasper Kreeft, and Marc Gerritsma. Physics-compatible discretization techniques on single and dual grids, with application to the poisson equation of volume forms. *Journal of Computational Physics*, 257:1394–1422, 2014. ISSN 0021-9991. doi: 10.1016/j.jcp.2013.08.005.
- [26] Christopher Beattie, Volker Mehrmann, Hongguo Xu, and Hans Zwart. Linear port-Hamiltonian descriptor systems. *Mathematics of Control, Signals, and Systems*, 30(4):17, Oct 2018. ISSN 1435-568X. doi: 10.1007/s00498-018-0223-3.
- [27] Robert J Guyan. Reduction of stiffness and mass matrices. *AIAA journal*, 3(2):380–380, 1965.
- [28] J. M. Sanz-Serna. Symplectic integrators for Hamiltonian problems: an overview. *Acta Numerica*, 1:243–286, 1992. doi: 10.1017/S0962492900002282.
- [29] Candan Güdücü, Jörg Liesen, Volker Mehrmann, and Daniel B. Szyld. On non-Hermitian positive (semi)definite linear algebraic systems arising from dissipative Hamiltonian DAEs. *SIAM Journal on Scientific Computing*, 44(4):A2871–A2894, 2022. doi: 10.1137/21M1458594.
- [30] K. C. Park, J. A. González, Y. H. Park, S. J. Shin, J. G. Kim, K. K. Maute, C. Farhat, and C. A. Felippa. Displacement-based partitioned equations of motion for structures: Formulation and proof-of-concept applications. *International Journal for Numerical Methods in Engineering*, 124(22):5020–5046, 2023. doi: 10.1002/nme.7334.
- [31] F. Rathgeber, D.A. Ham, L. Mitchell, M. Lange, F. Luporini, A.T.T. McRae, G.T. Bercea, G.R. Markall, and P.H.J. Kelly. Firedrake: automating the finite element method by composing abstractions. *ACM Transactions on Mathematical Software (TOMS)*, 43(3):24, 2017. doi: 10.1145/2998441.
- [32] zenodo/Firedrake-20231027.1. Software used in 'Finite Element Hybridization of port-Hamiltonian systems', oct 2023. URL <https://doi.org/10.5281/zenodo.10047121>.
- [33] T. H. Gibson, L. Mitchell, D. A. Ham, and C. J. Cotter. Slate: extending Firedrake's domain-specific abstraction to hybridized solvers for geoscience and beyond. *Geoscientific Model Development*, 13(2):735–761, 2020. doi: 10.5194/gmd-13-735-2020.
- [34] Jim Douglas and Jean E. Roberts. Global estimates for mixed methods for second order elliptic equations. *Mathematics of Computation*, 44(169):39–52, 1985. doi: 10.2307/2007791.
- [35] Marcus J. Grote, Anna Schneebeli, and Dominik Schötzau. Discontinuous Galerkin finite element method for the wave equation. *SIAM Journal on Numerical Analysis*, 44(6):2408–2431, 2006. doi: 10.1137/05063194X.

- [36] V. Jain, Y. Zhang, A. Palha, and M. Gerritsma. Construction and application of algebraic dual polynomial representations for finite element methods on quadrilateral and hexahedral meshes. *Computers & Mathematics with Applications*, 95:101–142, 2021. ISSN 0898-1221. doi: 10.1016/j.camwa.2020.09.022.
- [37] Yi Zhang, Joël Fisser, and Marc Gerritsma. A hybrid mimetic spectral element method for three-dimensional linear elasticity problems. *Journal of Computational Physics*, 433:110179, 2021. ISSN 0021-9991. doi: 10.1016/j.jcp.2021.110179.